9-1-2018

Investigation of an early season river flood pulse: Carbon cycling in a subtropical estuary

Benjamin J. Haywood
Louisiana State University

John R. White
Louisiana State University

Robert L. Cook
Louisiana State University

Recommended Citation

Haywood, B., White, J., & Cook, R. (2018). Investigation of an early season river flood pulse: Carbon cycling in a subtropical estuary. *Science of the Total Environment, 635*, 867-877. https://doi.org/10.1016/j.scitotenv.2018.03.379

HHS Public Access

Author manuscript

Sci Total Environ. Author manuscript; available in PMC 2019 September 01.

Published in final edited form as:

Sci Total Environ. 2018 September 01; 635: 867–877. doi:10.1016/j.scitotenv.2018.03.379.

Investigation of Early Season River Flood Pulse: Carbon Cycling in a Subtropical Estuary

Benjamin J. Haywood[1], **John R. White**[2], and **Robert L. Cook**[1,*]

[1]Department of Chemistry, Louisiana State University, Baton Rouge, United States

[2]Department of Oceanography & Coastal Sciences, Louisiana State University, Baton Rouge, United States

Abstract

The January 2016 Bonnet Carré Spillway (BCS) opening resulted in a large-scale Mississippi River (MR) flood discharge that qualitatively and quantitatively impacted the dissolved organic matter (DOM) cycling in the Lake Pontchartrain Estuary (LPE) located in Louisiana, USA. This early season flood event was a result of the delay of snow formation caused by warmer than normal watershed temperatures. During the diversion period and the subsequent weeks, the LPE water temperature remained lower than pre-flood water temperatures, suppressing carbon cycling. Following that period, the water temperature increased, leading to an increase in the rate of abiotic and biological carbon processing (i.e., mineralization, degradation, and consumption). There were multiple and abnormally high discharges into LPE from the northern tributaries, totaling 43% of the MR flood discharge. As a secondary DOM source, the northern tributaries discharge was qualitatively and quantitatively different from the discharge originating from the river or estuarine sources. The dominant DOM source was determined using satellite images in conjunction with UV-Vis, fluorescence EEMs, and PARAFAC indicators. Overall, the three sources (river, northern tributaries, and LPE) characteristics were identified by UV-Vis, fluorescence EEMs, and PARAFAC parameters, namely: i) spectral slope (S_{275}), serving as an indicator of lignin-like compounds' molecular weights, with a trend of MR > northern tributaries > LPE; ii) biological index (BIX), indicating freshness of DOM, with a trend of LPE > MR > northern tributaries; and iii) Fluorophore T intensity, serving as an indicator of the amount of terrestrial-like sourced DOM, with a trend of northern tributaries > LPE > MR. It was possible to identify DOM sources and monitor DOM transformation in the water column, increasing our understanding of DOM, carbon, and nitrogen ecological processing.

Graphical abstract

*Communicating Author: 307 Choppin Hall, Department of Chemistry, Louisiana State University, Baton Rouge, 70803: rlcook@lsu.edu.

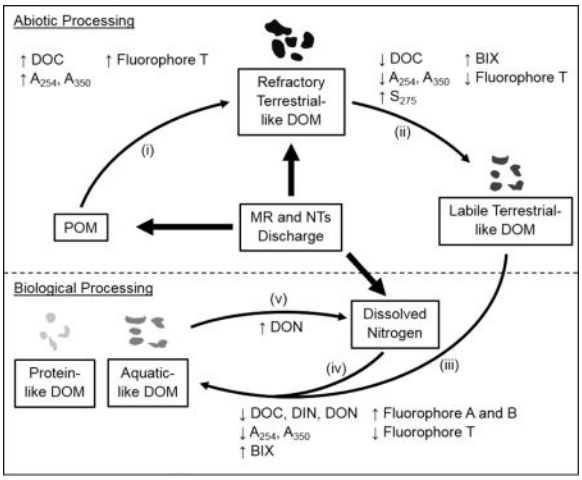

Keywords

Dissolved organic matter (DOM); Ultraviolet-Visible (UV-Vis); Fluorescence excitation emission matrices (EEMs); Parallel factor analysis (PARAFAC); Mississippi River; Lake Pontchartrain Estuary

1.0 Introduction

The Mississippi River (MR) has an extensive history of seasonal flooding, which benefits adjacent wetlands by bringing restorative water, sediments, and nutrients (Mossa, 1996). However, to prevent the flooding of New Orleans, Louisiana, the Bonnet Carré Spillway (BCS) is periodically opened to divert up to 20% of the flood stage flow from the MR—high in nutrients and terrestrial-like dissolved organic matter (DOM)—into the Lake Pontchartrain Estuary (LPE), which is low in nutrients and terrestrial-like DOM. These events can substantially influence the estuarine water column biogeochemistry (Kolic et al., 2014; Roy and White, 2012; White et al., 2009). The BCS openings have become increasingly necessary in recent years (Roy and White, 2012), allowing for a unique opportunity to study the dynamics of DOM in large estuaries subjected to large-scale introduction of freshwater carrying high terrestrial-like DOM and nutrient loads. These events can also inform managers on the effects of planned wetland restoration activities (large sediment diversion), including diverting the MR into adjacent estuarine and coastal wetland environments.

DOM is a heterogeneous collection of diverse products of decay that may be allochthonous or autochthonous in origin (i.e., terrestrial-like or aquatic-like), the composition of which depends on the parent organic matter and geochemical processes (Kolic et al., 2014; McKnight et al., 2001). DOM plays significant roles in natural and engineered systems, including controlling light attenuation, influencing metal and organic contaminants binding and overall bioavailability, and serving as a source of carbon and nutrients in the aquatic food web, and as a pH buffer (Cory and McKnight, 2005). Environmental scientists are increasingly emphasizing the geochemical and ecological roles of DOM in aquatic ecosystems (Weishaar et al., 2003). Determining DOM sources in estuaries and the factors

regulating its production, consumption, and transformation are critical for understanding the carbon cycle in these complex environments (Huguet et al., 2009).

The complex and heterogeneous nature of DOM makes it analytically challenging to study and characterize (Ohno and Bro, 2006). Spectroscopic techniques, such as ultraviolet-visible (UV-Vis) and fluorescence excitation emission matrices (EEMs), are useful tools for studying the concentration and characteristics of DOM in estuary systems (Coble, 1996; Cook et al., 2009; Kolic et al., 2014; Murphy et al., 2010). Indices calculated from UV-Vis absorbance at various wavelengths and fluorescence EEMs are used as indicators of DOM concentration (i.e., aromatic and lignin-like carbon) and characteristics (i.e., lignin-like compounds' molecular weights (MW) and DOM freshness) (Cook et al., 2009; Kolic et al., 2014). Additionally, with the use of multi-way modeling analysis, with parallel factor analysis (PARAFAC) being the most commonly implemented, the intensity and identity of individual fluorophores within a DOM sample can be determined (Murphy et al., 2013).

The January 2016 large-scale MR discharge into LPE was the earliest in its 91 years of operation, with the previous most recent three opening events having occurred March 17-April 18, 1997, April 11- May 8, 2008, and May 9-June 20, 2011 (Roy and White, 2012). This event can be viewed as a winter versus the typical spring discharge event. However, due to the ever-changing climate, such early discharges could be expected to become more common in the future. Therefore, previous understanding of carbon dynamics during spring MR discharges into LPE, outlined in Roy and White, 2012 and Kolic et al., 2014, may not apply due to a shifting range of seasonally based norms in water temperature, precipitation, and length of exposure to solar radiation. This study of a winter river flood discharge applied a combination of dissolved carbon and nitrogen, UV-Vis, and fluorescence EEMs along with PARAFAC analysis to understand the carbon dynamics in terms of DOM concentration, characteristic, and transformations within the LPE during and after the discharge event. These measures were utilized to understand how dissolved organic carbon cycling may change in the future as a result of a shifting climate.

2.0 Methods

2.1 Sample Collections

The Bonnet Carré Spillway (BCS) control structure is situated along the north bank of the Mississippi River, located 52 km up river from New Orleans. The spillway system is connected to Lake Pontchartrain Estuary by low-lying floodway 4.10 km wide and 8.7 km in length with an overall design capacity of 7100 $m^3 s^{-1}$ (USACE, 2016). On January 10, 2016, the BCS was opened due to the anticipated flood stage of the Mississippi River. The BCS was closed on January 31, 2016, once the river had crested.

Sampling was performed at eleven sites along a singular 29.36 km-long transect, starting at the BCS opening and extending to the center of LPE, with two sites close to the opening (D1 and T1) and the rest of the sites (T11-T19) located in 3.0 km intervals (Figure 1). Samples were collected on specific dates to represent: i) pre-opening (January 8, 2016), ii) during opening of BCS (January 15, 24, and 29, 2016), and iii) post opening of BCS (February 5, 19, and 26; March 25; and May 5, 2016) (Figure 2). Due to safety concerns resulting from

poor weather conditions, samples were not collected at sites D1 on January 8, 2016, T18 and T19 on February 26, 2016, or D1 on May 5, 2016. Water sampling was performed following the procedure after Kolic et al., 2014, with samples collected 10 cm below the surface of the water at each site. To ensure continued quality control, field triplicates were collected and analyzed at one site per sampling day throughout the study. Water temperatures were measured *in situ* using a handheld YSI (Model 556). Water samples were collected by inverting an acid-washed polyethylene bottle and washing three times with site water. Samples were then filtered (using a 0.45 μm × 13 mm Nylon syringe filter) on site into ashed 20 mL borosilicate glass scintillation vials with Poly-Seal cone caps. The samples were then stored on ice during transport, refrigerated at 4 °C, and shielded from light until analysis.

2.2 Ultraviolet-Visible Spectroscopy (UV-Vis)

The UV-Vis absorbance spectra were collected from 200 to 600 nm using a 0.5 nm bandpass and a 1 cm quartz cell, on a Cary 100 Spectrophotometer. To minimize temperature effects, samples were allowed to warm to room temperature and shielded from light prior to analysis. The resulting UV-Vis absorption spectra for DOM samples are typically featureless, but several indicators have been developed and used to analyze concentration and characteristics of the DOM (Weishaar et al., 2003). In-depth descriptions of UV-Vis indicators used in this study are presented in Table 1. Field triplicates of UV-Vis measurements resulted in percent standard deviation of < 1 %. The data for each indicator and their specific percent standard deviations are presented in Supplementary Information S1.

2.3 Fluorescence Excitation Emission Matrices (EEMS)

Fluorescence EEMs were collected using a 1 cm quartz cell with excitation wavelengths of 250 to 550 nm and emission wavelengths of 250 to 600 nm with 5 nm increments for both on a Spex Fluorolog-3 spectrofluorometer. Along with sample EEMs, blank EEMs of Milli-Q water were collected daily. As with the UV-Vis samples, temperature effects were minimized as described above. Prior to indicator calculation and PARAFAC modeling, the EEMs were pre-processed following procedures outlined in Murphy et al., 2010. In-depth descriptions of the fluorescence EEMs indicators used in this study are presented in Table 1. Field triplicates of fluorescence measurements resulted in average percent standard deviation of 0.50 %. The data for the indicator are presented in Supplementary Information S1.

2.4 Parallel Factor Analysis (PARAFAC) Modeling

The pre-processed sample data were arranged into a three-way array with 114 samples, 61 excitation wavelengths in 5 nm increments ranging from 250 to 550 nm, and 71 emission wavelengths in 5 nm increments ranging from 250 to 600 nm. The fluorescence intensity was converted from arbitrary unites (A.U.) to Raman unites (R.U.) before PARAFAC analysis. The PARAFAC analysis was performed with MATLAB R2015a (Math Works, Inc., Cambridge, MA) software program, utilizing open source drEEM toolbox version 2.0 (Murphy et al., 2013). The appropriate number of components for the dataset was determined using outlier identification and method validation techniques (i.e., least square fit and split-half analysis) following methods outlined in Murphy et al., 2013, with the best fit model having an explained variance of > 95%. The identities of the components determined

in the model were verified through comparison to previously identified component models using OpenFluor (DOM fluorescence spectral database) (Murphy et al., 2014). Field triplicates of PARAFAC analysis resulted in percent standard deviation of < 1.2 %. The results of PARAFAC analyses, split-half analysis, and their specific percent standard deviation can be found in Supplementary Information S2.

2.5 Satellite Images

Satellite images for each field sampling date were provided by the Louisiana State University Earth Scan Laboratory. The flow pattern of the discharge originating from the northern tributaries and from the Mississippi River (MR) that occurred within Lake Pontchartrain Estuary (LPE) were estimated using the satellite images. The distinct reflectance of each discharge's plume (i.e., northern tributaries and MR) compared to LPE allowed for the monitoring of the movement, mixing, and impact of the discharges on different sites across the sampling transect over the course of the sampling period and was further refined by spectroscopic data (Supplementary Information S3).

2.6 Dissolved Carbon and Nitrogen Analyses

Water samples were collected using acid-washed polyethylene bottles, placed on ice, and returned to the laboratory immediately for processing. Samples were then vacuum-filtered through 0.45 μm membrane filters and stored in ashed glass vials with Teflon-coated caps at 4 °C. Prior to analysis of DOC and dissolved organic nitrogen (DON), samples were acidified with concentrated hydrochloric acid (0.2 mL HCl in 40 mL sample) and allowed to degas the inorganic carbon. The DOC and DON were measured on a Shimadzu TOC-V CSN analyzer. Dissolved inorganic nitrogen (DIN) was measured by analyzing the water samples for NO_3-N (USEPA Method 353.2), and NH_4-N (USEPA Method 350.1) (USEPA, 1993) within 24 hours on a Seal Analytical (Mequon, Wisconsin) AQ2+discrete analyzer using standard colorimetric methods. Quality control measures included analyses of standards along with each run, field triplicates, laboratory duplicates, and matrix spikes. Field triplicate samples resulted in percent standard deviation of less than 3 % for dissolved carbon and nitrogen measurements. The data for dissolved carbon and nitrogen measurements and their specific percent standard deviation are presented in Supplementary Information S1.

2.7 Mississippi River and Northern Tributary Discharge Data

The Mississippi River discharge was determined from data collected by the United States Army Corps of Engineers (USACE, 2016). The discharge from the northern tributaries to LPE was determined using data collected by the United States Geological Survey (USGS) at: the Amite River near Denham Springs (USGS Station 7378500), the Tangipahoa River at Robert (USGS Station 7375500), the Tchefuncte River near Folsom (USGS Station 7375000), the Tickfaw Rivers at Holden (USGS Station 7376000), and the Natalbany River at Baptist (USGS Station 7376500). The daily discharge of each of the five rivers was summed, giving the total daily discharge for the months of January-May 2016 (USGS, 2016).

3.0 Results and Discussion

3.1 Satellite Images, DOM Sources, and Indicators

Over the study period, several factors changed (i.e., water temperature, dissolved carbon and nitrogen concentrations, and DOM concentration and characteristics) in the Lake Pontchartrain Estuary (LPE) due to the Mississippi River (MR) and northern tributaries discharge, and needed to be accounted for before the measurements could be analyzed. Satellite images illustrated the plume extent from the MR discharge into LPE. Additionally, a secondary plume with a different reflectance, entering from the north shore of Lake Pontchartrain, was determined to be the discharge from the northern tributaries. The northern tributaries' discharge intersected the sampling transect at various locations over time (Supplementary Information Figure S3-1). Quantitatively, there was a single MR discharge pulse totaling 6.93 km^3 for the 22 days when the Bonnet Carré Spillway (BCS) was open, and multiple pulses of varying amounts from the northern tributaries' discharge over the course of the study period totaling 2.96 km^3 (Figure 2). This led to a temporal mixing of three different DOM pools, namely the ambient LPE, MR, and northern tributaries. The assignment of DOM sources and mixing was initially determined by satellite imagery and the visual difference in reflectance of water surrounding each site along the transect. The assignments were later refined through statistical comparison ($p<0.05$) of the mixing and dominant DOM sources using fluorescence-determined biological index (BIX) values during each sampling day (Table 2). An example of this process is provided in Supplementary Information Figures S3-2 and S3-3. Pure DOM sources were determined based on each discharge event, and the identified pure DOM sources had UV-Vis, fluorescence EEMs, and PARAFAC indicators with significantly different ($p<0.05$) mean values (Table 3).

For the purposes of the discussion to follow, we differentiate between abiotic and biological processes affecting carbon cycling, where i) abiotic processes are defined as processes occurring outside the cell and refer to DOM degradation (such as photo- and extracellular enzymatic cellular degradation); and ii) biological processes are defined as those occurring inside the cell and refer to DOM consumption and/or production (e.g., aquatic growth).

3.2 DOM Before MR Discharge (January 8, 2016)

3.2.1 Weather and Discharge Conditions—Two days prior to the MR discharge, water samples were collected along the ~30 km transect and are considered to be "normal" or representative of pre-flood conditions with minimal (0.0065 km^3) northern tributary discharge impact (Figure 2). The water temperature on January 8, 2016 ranged from 12.33 to 13.20 °C, with a spatial trend of decreasing water temperature across the transect (Figure 3). The aforementioned water temperature range has been previously shown to favor abiotic over biological processing of the DOM (Arnosti and Jørgensen, 2003; Hernes et al., 2008; Weston and Joye, 2005).

3.2.2 Dissolved Carbon and Nitrogen and Trends in Spectroscopic Indicators —There was no change in DOC concentration across the transect prior to the river discharge event (Figure 4). Whereas, DIN and DON indicated a leakage of nitrogen-rich water from

the BCS by a trend of decreasing concentration with increasing distance, to the east (along the transect, for the remainder of the discussion) from the spillway (Figure 4). The UV-Vis indicators show an introduction and, subsequently, abiotic processing of aromatic carbon and lignin, through the decreasing concentration of aromatic carbon (A_{254}) and lignin-like carbon (A_{350}) and decreasing lignin-like compounds' molecular weight (inverse to S_{275} value) along the transect from the sites near the spillway eastward into the center of the LPE (Figure 5) (Fichot and Benner, 2012). The BIX values indicate a trend of abiotic and biological processing with less fresh DOM (low BIX value) at sites near the BCS and more fresh DOM (high BIX value) at sites approaching the center of LPE (Figure 6) (Huguet et al., 2009). The DOM obtained from the sites near the BCS inflow is refractory in nature, as indicated by the high molecular weight (S_{275}) of its lignin-like compounds' content, and less fresh, as suggested by the low BIX values. Additionally, the DOM obtained from the sites closer to the center of the LPE identifies as labile (i.e., lignin-like compounds with low molecular weight (S_{275}) and fresher DOM (BIX)) (Fichot and Benner, 2012; Huguet et al., 2009). The PARAFAC-determined F_{max} intensity was dominated by humic-like autochthonous (aquatic-like, Fluorophore A) sourced DOM that is typical for estuaries like the LPE (Coble, 1996; Murphy et al., 2010). The other determined fluorophores support the abiotic processing and indicate biological processing through a trend of higher intensity of humic-like allochthonous (terrestrial-like, Fluorophore T) sourced DOM at sites near the BCS and a higher intensity of protein-like autochthonous (Fluorophore B) sourced DOM at sites near the center of the LPE (Figure 7).

3.2.3 Ecological Significance—From an ecological stand point, the carbon in the LPE under the pre-flood event conditions can be described as dominated by aquatic-like sourced DOM, with MR-sourced DOM leaking from the BCS into the LPE (Kolic et al. 2014) and being both abiotically and biologically processed along the transect towards the center of the LPE. Due to the DOM leaking in from the BCS, sites close to the BCS (D1 and T1) contain high concentrations of nitrogen and refractory terrestrial-like DOM. As the water moves along the transect, eastward, abiotic processing degrades the refractory terrestrial-like DOM into labile terrestrial-like DOM. This process and the indicator changes are represented in Figure 8 by Transformation (ii). The yielded labile terrestrial-like DOM, along with the dissolved nitrogen (DIN and DON), are consumed through biological processing, resulting in the release of protein-like, and production of aquatic-like, DOM. This process and the associated indicator changes are represented in Figure 8 by Transformations (iii) and (iv). An apparent conservation of DOC is seen in the maintenance of the DOC concentration along the transect.

3.3 DOM During the MR Diversion (January 15, 2016 through January 29, 2016)

3.3.1 Weather and Discharge Conditions—Sampling was performed on January 15, 24, and 29 2016; with a total MR discharges of 1.27 km^3 (January 10 - 15, 2016), 5.56 km^3 (January 10 - 24, 2016), and 6.85 km^3 (January 10 - 29, 2016), and northern tributaries discharge reached totals of 0.056 km^3 (January 10 - 15, 2016), 0.142 km^3 (January 10 - 24, 2016), and 0.231 km^3 (January 10 - 29, 2016) (Figure 2). Overall, the MR discharge introduced more fresh water than that from the northern tributaries during each sampling and thus is the dominant DOM source for this period (Table 2). During the diversion event, the

MR discharge lowered the water temperature, which ranged from 5.78 °C, for sites closer to the BCS, to 11.94 °C, for sites further away from the BCS (Figure 3). A decrease in water temperature has been previously shown to limit carbon cycling processes (Arnosti and Jørgensen, 2003; Hernes et al., 2008; Weston and Joye, 2005).

3.3.2 Dissolved Carbon and Nitrogen Trends—A trend of increasing DOC concentration and decreasing DIN and DON concentrations along the transect was constant over the sampling period (Figure 4). The DOC, DIN, and DON values did not vary over this sampling period, indicating a lack of biological processing during the diversion event. With the MR-dominated sites having the lowest DOC and highest DIN and DON concentrations compared to the other sources during this period and the allochthonous (terrestrially-sourced) refractory DON being higher in concentration than the biologically available DIN (Riekenberg et al., 2015).

3.3.3 Trends in Spectroscopic Indicators—There was a trend of increasing concentrations of aromatic carbon (A_{254}) and lignin-like carbon (A_{350}) as well as a decrease in lignin-like compound MW (S_{275}) along the transect (Figure 5). This trend was determined to result from the influence of the different DOM sources at each site along the transect. The MR DOM-dominated sites (D1 and T1-T12) had the lowest concentration of aromatic carbon (A_{254}), total lignin-like carbon (A_{350}) as well as lignin-like compounds with the highest MW (S_{275}) compared to the other source-dominated sites (Figure 5). A decrease in lignin-like compounds' MW (S_{275}) during this sampling period indicated abiotic DOM processing in the MR DOM-dominated sites. Utilizing the S_{275} data, the following trend in terms of lignin-like compounds' MW within the different DOM sources can be established: MR > northern tributaries > LPE. DOM freshness, as determined by BIX data (Figure 6), was found to be strongly dependent on the dominant DOM source, with the following trend in DOM freshness: LPE > MR > northern tributaries (Table 3). The DOM freshness (BIX) increased, over the diversion period, for sites close to the spillway (D1 and T1-T12) indicating an abiotic processing of the MR DOM. Analysis of the combination of S_{275} and BIX data supports the conclusion that the transformation of refractory to labile DOM though abiotic processing was the dominant mode of processing during the MR diversion event.

PARAFAC analysis of the fluorescence EEM data showed that F_{max} intensity of humic-like autochthonous (Fluorophore A) and allochthonous (Fluorophore T) sourced DOM was dependent on the dominant DOM source at each site (Table 3). The MR DOM-dominated sites had the lowest intensity for both Fluorophore A and T, compared to northern tributaries and LPE mixed DOM sites (Figure 7). Processing of the MR allochthonous DOM fraction was indicated by the decrease in the intensity of Fluorophore T. Throughout the MR diversion between January 15 and 29, 2016, biological processing was indicated by an increase in the intensity of protein-like autochthonous (Fluorophore B).

3.3.4 Ecological Significance—Overall, during the diversion of the MR, DOM was determined to be a mixture of terrestrial-like and aquatic-like sourced DOM, with an overall lower than expected concentration of DOC, aromatic carbon, and lignin-like carbon, and higher concentrations of DIN and DON (Kolic et al., 2014). During the diversion event, abiotic processing of the refractory terrestrial-like DOM from the MR discharge into labile

terrestrial-like DOM was determined to occur in sites close to the spillway by the steady decrease in lignin-like compounds' MW, increase in freshness, and decrease in the intensity of terrestrial-like DOM (Figure 8; Transformation (ii)). Additionally, biological processing during the diversion was determined in the eastern sites of the transect by the decrease in the intensity of terrestrial-like sourced DOM and an overall increase in the intensity of protein-like sourced DOM (Figure 8; Transformation (iii)). Based on the relatively modest changes in the above-mentioned indicators, it can be concluded that overall ecological changes (especially biological processing) were suppressed by the low water temperature across the transect during the MR diversion period.

3.4 Dynamic Change of DOM After the MR Discharge (February 5, 2016 through February 26, 2016)

3.4.1 Weather and Discharge Conditions—After the closing of the spillway, sampling was performed on February 5, 19, and 26, 2016; with the northern tributaries discharge having reached a total of 0.411 km^3 (January 10 - February 5, 2016), 0.582 km^3 (January 10 - February 19, 2016), and 0.751 km^3 (January 10 - February 26, 2016) (Figure 2). Overall, during this period, the MR discharge was still the dominant DOM source along the transect, with only a few sites in the center of the transect (T13-T16) being impacted by the northern tributaries discharge (Table 2). The water temperature ranged from 10.90 to 15.93 °C, with an increase in water temperature during each consecutive sampling (Figure 3). Increasing water temperature during this time period, compared to pre-flood conditions, is predicted to increase the rate of both the abiotic and biological carbon cycling processes of the DOM introduced during the MR diversion.

3.4.2 Dissolved Carbon and Nitrogen Trends—During this sampling period, the concentration of DOC along the transect was indicative of the dominant DOM source for each site, with northern tributaries DOM-dominated sites maintaining a higher concentration of DOC throughout the sampling period, compared to the other sites (Figure 4). The concentration of DOC in the MR, MR/LPE mixed, and LPE-dominated DOM sites were much higher during this period than for the previous periods. This internal increase in DOC concentration is consistent with the abiotic processing of river-derived particulate organic matter (POM) that remained relatively undegraded during the diversion event due to the cold river water temperatures (Arnosti and Jørgensen, 2003; Weston and Joye, 2005). This is supported by the measured decrease in total suspended solid concentration during this time period (Supplementary Information, Table S4-1). The concertation of DOC in MR, MR/LPE mixed, and LPE-dominated DOM sites reached the high mark on February 19, 2016 after which it decreased through the last day of this sampling period, indicating further DOM processing.

The DIN concentration decreased between January 29 and February 19, 2016, and leveled off by February 26, 2016 (Figure 4). However, the DON concentration showed an increase during the February 5, 2016 sampling, decreased during the February 19, 2016 sampling, and increased during the February 26, 2016, sampling. This pattern of DIN and DON concentrations indicates an initial consumption of more bio-available DIN during January 29 - February 19, 2016 period by biological processing (Riekenberg et al., 2015), with a

delayed consumption of refractory DON during February 5 - 19, 2016 period (Zehr and Ward, 2002). The DIN consumed by the biological processing was likely converted into DON, leading to the increased DON content seen in the February 26, 2016 sampling (Bargu et al., 2011; Ghosh and Leff, 2013; Roy et al., 2013; White et al., 2009).

3.4.3 Trends in Spectroscopic Indicators—During this period, the northern tributaries-dominated DOM sites had the higher concentration of aromatic carbon (A_{254}) and lignin-like carbon (A_{350}) and maintained similar values of lignin-like compounds' MW (S_{275}) compared throughout the sampling period (Figure 5), indicating a consistent water input from the northern tributaries (Table 3). Sampling during the February 5 - 19, 2016 period revealed that the MR DOM-dominated sites (D1 and T1-T12) had an increase in the concentration of the aromatic carbon (A_{254}) and lignin-like carbon (A_{350}). This trend of internal increases in the concentration of the aromatic carbon (A_{254}) and lignin-like carbon (A_{350}) supports the introduction of the MR POM and the delayed abiotic processing predicted by the DOC measurements. By February 26, 2016, the abiotic processing of the POM has been completed, as indicated by the decrease in concentration of DOC, aromatic carbon, and lignin-like carbon, and a decrease in lignin-like compounds' MW.

Fluorescence data further support these observations, with the BIX values during this period being indicative of the specific DOM source (Table 3). The decrease in freshness between February 5 and 19, 2016 supports the assertion of abiotic processing of POM into refractory DOM (Figure 6). The increase in freshness between February 19 and 26, 2016 also supports the curtailing of the POM abiotic processing.

The F_{max} intensities of aquatic-like (Fluorophore A) and terrestrial-like (Fluorophore T) sourced DOM during these samplings show trends specific to the dominant DOM source at each site (Table 3), whereas intensities of protein-like autochthonous (Fluorophore B) were shown to be dependent only on the sampling day (Figure 7). During the period from February 5 to 26, 2016, the abiotic processing of MR POM is supported by the increased amount of terrestrial-like DOM, as indicated by the Fluorophore T intensity. The aquatic-like and protein-like sourced DOM reached their respective highest concentrations between February 19 and 26, 2016, as indicated by the Fluorophore A and Fluorophore B intensities, respectively. The significant increase of Fluorophore A and B intensities indicates an increase in biological processing, as expected due to the increased water temperature, the surplus of dissolved nitrogen (initially DIN), and the presence of labile terrestrial-like DOM.

3.4.4 Ecological Significance—Consistent discharge from the northern tributaries during this period resulted in a constant DOM concentration and characteristics of the northern tributaries DOM-dominated sites (T13-T16) (Table 2). Contrary to this, the DOM from the MR discharge-dominated sites (D1 and T1-T12) underwent increased rates of carbon cycling processes due to increased water temperature. During the sampling days of February 5 to 19, 2016, the MR-introduced POM was subject to increased rates of abiotic processing, resulting in a release of refractory terrestrial-like DOM (Figure 8; Transformation (i)). This process is indicated by increased DOC, increased aromatic carbon and lignin-like carbon concentration, and heightened intensity of terrestrial-like sourced DOM. Between February 19 and 26, 2016, the newly-produced and introduced refractory

terrestrial-like DOM was further abiotically processed into labile terrestrial-like DOM, as illustrated in Figure 8 by Transformation (ii). This process is indicated by the decrease in DOC, aromatic carbon, and lignin-like carbon concentrations, a decrease in lignin-like compounds' MW, and an increase in freshness (Arnosti and Jørgensen, 2003; Hernes et al., 2008; Stedmon and Markager, 2005; Weston and Joye, 2005). Biological processing of the labile terrestrial-like DOM and bio-available DIN resulted in a decrease in the DIN concentration between February 5 and 19, 2016 and an increase in the intensity of autochthonous-sourced DOM between February 19 and 26, 2016 (Figure 8; Transformations (iii) and (iv)) (Ghisaidoobe and Chung, 2014). The inorganic nitrogen consumed between February 5 and 19, 2016 was converted to organic nitrogen and released during biological processing, resulting in the increased concentration of DON between February 19 and 26, 2016 (Figure 8; Transformation (v)) (Coble et al., 1998; Ghosh and Leff, 2013). The increase in biological processing is predicted to be quenched after the surplus dissolved nitrogen and labile terrestrial-like DOM were mostly consumed.

3.5 DOM from the Northern Tributaries Discharge (March 25, 2016)

3.5.1 Weather and Discharge Conditions—Between February 26 and March 25, 2016, the northern tributaries discharge reached a total of 1.44 km^3, consisting of 48.5% of the 2.96 km^3 total northern tributaries discharge during the sampling period (Figure 2). This large water input was the result of a storm event, triggering a shift to the northern tributaries as the dominant DOM source in LPE on March 25, 2016. The higher water temperature during this period, ranging between 16.08 °C to 18.50 °C (Figure 3), would lead to the prediction of an increase in the rates of carbon cycling processes.

3.5.2 Dissolved Carbon and Nitrogen Trends—The DOC concentrations showed an increasing trend in concentration, while DIN and DON concentrations decreased with increasing distance from the BCS (Figure 4). The concentration of DOC, DON, and DIN at sites adjacent to the BCS (D1 and T1) are similar to those seen during the MR diversion event (between January 10 to 31, 2016) and are attributed to river water leakage through the BCS (Kolic et al., 2014). The decreased in DOC concentration seen between February 26 and March 25, 2016 is postulated to be the result of both abiotic and biological carbon cycling processes. The DIN and DON trends along the sampling transect are identical to those measured prior to the flood event and are indicative of biological processing. The northern tributaries DOM-dominated sites had no change in the concertation of nitrogen, indicating little change in the DOM originating from the northern tributaries discharge.

3.5.3 Trends in Spectroscopic Indicators—Sites D1 and T1 (adjacent to BCS) had a lower concentration of aromatic carbon (A_{254}) and lignin-like carbon (A_{350}), as well as lignin-like compounds with higher MW (S_{275}), compared the rest of the transect, being also indicative of a continued river water leakage through the spillway structure even after its closure on January 31, 2016 (Figure 5). From February 26 to March 25, 2016, the northern tributaries and LPE mixed sites showed a decrease in the aromatic carbon and lignin-like carbon concentration and a decrease in lignin-like compounds' MW, indicating abiotic processing. In support of this predicted abiotic processing was the increase in the freshness of the DOM (BIX) in northern tributaries and LPE mixed sites between February 26 and

March 25, 2016. DOM freshness for sites D1 and T1 during this sampling matched that of the sites during MR diversion, further indicating leakage from the BCS (Figure 6). DOM freshness for all sites was strongly dependent on the dominant DOM source at each site (Table 3).

The above UV/Vis observations are further collaborated by fluorescence measurements. The F_{max} intensities of aquatic-like (Fluorophore A) and terrestrial-like (Fluorophore T) sourced DOM had trends specific to the dominant DOM source at each site (Table 3). Compared to the rest of the sites, the spillway adjacent sites (D1 and T1) showed lower intensity for both Fluorophore A and Fluorophore T, which, once again, was indicative of the MR DOM dominating the DOM pool of these sites due to BCS leakage (Figure 7). Continual abiotic processing is indicated for the northern tributaries and LPE mixed sites via the decrease in terrestrial-like (Fluorophore T) DOM from February 26 through March 25, 2016. During this period, there was a suppression of biological processing, as indicated by the decrease in aquatic-like (Fluorophore A) and protein-like (Fluorophore B) DOM intensities.

3.5.4 Ecological Significance—Dissolved carbon and nitrogen, UV-Vis, fluorescence EEMs, and PARAFAC indicators of sites D1 and T1 (adjacent to BCS) have identical values, compared to those of the same sites during MR diversion. These measured values are determined to be due to higher vegetation density at the BCS inflow and potentially minor, but constant, MR discharge leaking through the BCS structure that was first identified by Kolic et al., 2014. Additionally, abiotic processing of refractory terrestrial-like DOM in the northern tributaries and LPE mixed site into labile terrestrial-like DOM was determined to occur (Figure 8; Transformation (ii)). Comparing samplings on February 26 and March 25, 2016, the measured values show a retardation of biological processing (Figure 8; Transformations (iii) and (iv)).

3.6 DOM After the Northern Tributaries Discharge (May 5, 2016)

3.6.1 Weather and Discharge Conditions—By May 5, 2016, the northern tributaries discharge had reached a total of 2.96 km^3 (Figure 2). At the same time, the water temperature increased significantly and ranged between 22.69 °C and 23.48 °C (Figure 3). During this time period, the northern tributaries discharge was the dominant DOM source for sites T14-T17 (Table 2).

3.6.2 Dissolved Carbon and Nitrogen Trends—The DOC concentration increased from March 25 through May 5, 2016, and was predicted to be the result of a DOC build-up from multiple northern tributaries discharges during this period (Figure 4). Biological processing reduced the concentration of DIN to “normal” (pre-flood, January 8, 2016) concentration levels, indicating near complete consumption of the readily bio-available DIN introduced during MR diversion by biological processing. This biological processing converted the DIN to DON and resulted in DON concentration on May 5, 2016 being higher than the levels considered to be “normal” for LPE (Figure 4).

3.6.3 Trends in Spectroscopic Indicators—Using lignin-like compounds’ MW (S_{275}), sites T1 and T14-T17 were predicted to be dominated by northern tributaries DOM (Table

3). The other sites along the transect show an increase in the concentration of aromatic carbon (A_{254}) and lignin-like carbon (A_{350}) from March 25 until May 5, 2016, supporting the northern tributaries DOM build-up (Figure 5). The lack of apparent change in lignin-like compounds' MW (S_{275}) at other sites from March 25 through May 5, 2016, indicates a decrease in abiotic processing. The DOM freshness (BIX) for site T1 is similar to pre-flood values and indicates LPE as the source. The DOM freshness of sites T14-T17 is in agreement with above, with satellite images indicating an impact from the northern tributaries discharge (Figure 6). The other sites show no apparent change in DOM freshness (BIX) between March 25 and May 5, 2016, indicating a decreased rate of abiotic and biological processing.

The F_{max} intensities of Fluorophore A and T match the above trends, with the highest values measured at sites T1 and T14-T17, indicating northern tributaries as the dominant DOM source (Table 3). The retardation of abiotic processing of the terrestrial-like DOM pool put forward above is supported by an increase in the intensity of the terrestrial-like (Fluorophore T) DOM component between March 25 and May 5, 2016 (Figure 7). The modest increase in intensities of aquatic-like (Fluorophore A) and protein-like (Fluorophore B) sourced DOM components between March 25 and May 5, 2016, compared to changes in other periods, indicates that biological processing was still occurring.

3.6.4 Ecological Significance—Ecologically, by this time, the biological processing had slowed, as indicated by the low DIN and DON concentrations and the decreased aquatic-like and protein-like sourced DOM components in the overall DOM pool. Furthermore, the rate of the abiotic processing had largely decreased, as indicated by the increased concentration of DOC, aromatic carbon, and lignin, limited change in the lignin-like compounds' MW, and increased terrestrial-like sourced DOM component in the overall DOM pool between March 25 and May 5, 2016. Overall, during this period, there was an apparent balancing of the DOM characteristics, which is indicative of a minimal carbon cycling. Using the indicator values determined for each dominant DOM source (Table 3), sites T14-T17 were dominated by northern tributaries discharge. By contrast, site T1 was dominated by a mixture of northern tributaries and LPE DOM.

3.7 Synthesis

The total mass of DOC, DON, and DIN inputs from MR and northern tributaries discharges were calculated by: i) using DOC, DON, and DIN inputs concentrations at the sites dominated by these inputs during the sampling, ii) averaging these values over the course of each respective discharge event, and iii) multiplying by the volume of the total discharge for each event. The Mississippi River flood discharge introduced 120,000 metric tons of DOC, 13,000 metric tons of DIN, and 24,000 metric tons of DON in just less than a month in January 2016. The northern tributaries discharge introduced 71,000 metric tons of DOC, 1,300 metric tons of DIN, and 5,700 metric tons of DON over the course of the study from January - May 2016. Consequently, in a much shorter period of time, the MR introduced 1.7 times more DOC, 10 times more DIN, and 4.2 times more DON than the northern tributaries did but both inputs had a major impact on the water column of this shallow estuary.

The carbon cycling processing of these DOM inputs into LPE can be described by: a) abiotic processing (i.e., photo- and extracellular enzymatic degradation); and b) biological processing (i.e., aquatic activity) during and after the 2016 large-scale MR discharge (January 10 to 31, 2016) (Figure 8). The abiotic processing of the MR-introduced particulate organic matter (POM) into a pool of refractory terrestrial-like DOM is expressed by indicators in Figure 8 by Transformation (i). This transformation is highlighted by the lack of outside input and an increase in the concentration of terrestrial-like organic matter, which indicates the breakdown of terrestrial-like particulate organic matter into refractory terrestrial-like DOM. The further abiotic processing of this refractory terrestrial-like DOM, or that inputted by the MR or northern tributaries discharge, into labile terrestrial-like DOM is expressed by indicators in Figure 8 by Transformation (ii). Transformation (ii) represents the decrease in concentration of terrestrial-like organic matter and is corroborated by the decrease in the MW of lignin-like compounds (inverse S_{275} value), which has been previously demonstrated to be the result of photodegradation (Fichot and Benner, 2012).

The biological processing seen occurring throughout the sampling period is expressed by indicators in Figure 8 by Transformations (iii) and (iv). Transformations (iii) and (iv) represent the decrease in concentration of both labile terrestrial-like DOM and dissolved carbon and nitrogen, as well as the production of aquatic-like and protein-like DOM. These transformations are identified by the increase in the intensity of the aquatic-like (Fluorophore A) and protein-like (Fluorophore B) sourced DOM, with the last biological processing transformation being the result of a feedback loop in the release of DON (Figure 8; Transformation (v)).

4.0 Conclusion

The changes in source and carbon cycling processes of DOM, resulting from the MR (120,000 metric tons of DOC, 13,000 metric tons of DIN, and 24,000 metric tons of DON) and northern tributaries (71,000 metric tons of DOC, 1,300 metric tons of DIN, and 5,700 metric tons of DON) inputs into the LPE were identified over time by using dissolved carbon and nitrogen, UV-Vis, fluorescence EEMs, and PARAFAC indicators and further supported by satellite imagery. The general relationship of the three DOM sources (MR, northern tributaries, and LPE) can be described by characteristic differences indicated by significant ($p<0.05$) difference in values of: i) lignin-like compounds' molecular weight (S_{275}) with a trend of MR > northern tributaries > LPE; ii) DOM freshness (BIX) with a trend of LPE > MR > northern tributaries; and iii) the intensity of terrestrial-like sourced DOM (Fluorophore T, intensity) with a trend of northern tributaries > LPE > MR (Table 3). The mixed sites indicate an average of the DOM sources.

Overall, the carbon cycling processing was suppressed by the low water temperatures of the river during the earlier samplings. The higher water temperatures, post-spillway closure, led to abiotic and biological processing of the MR-introduced POM, DOM, and dissolved carbon and nitrogen. Later in March, the abiotic and biological processing slowed, indicating the completed processing of the MR inputs. The northern tributaries discharge then became the major source of DOM as well as of dissolved carbon and nitrogen. By May, the DOM in LPE is shown to be characteristically similar to that of the pre-flood conditions.

However, the combined effects of the two discharges resulted in the LPE having a higher concentration of DOC, DON, aromatic carbon, and lignin-like carbon, with a lower concentration of DIN when compared to pre-flood conditions. This unusually early MR flood event resulted in an increase of abiotic and biological processing of the newly introduced carbon pools which, in turn, led to a marked increase of carbon and DON in the LPE (Figure 8), and potentially significant ramifications for coastal systems' primary production. The type of an early season flood event that was the center of this project was caused by warmer than normal wintertime watershed air temperatures and is likely to become more common as current global climate change trend continues. Thus, understanding the impact these early flooding events have on the ecosystem will become increasingly important and essential in the near future.

Supplementary Material

Refer to Web version on PubMed Central for supplementary material.

Acknowledgments

This work was supported by the National Science Foundation under grants CHE-1411547 and OCE-1636052 and the NIEHS Superfund Research program for Louisiana State University under grant 2P42ES013648-03. We thank Dr. Nan Walker at Louisiana State University Earth Scan Laboratory for providing the MODIS satellite images.

References

Arnosti C, Jørgensen B. High activity and low temperature optima of extracellular enzymes in Arctic sediments: implications for carbon cycling by heterotrophic microbial communities. Marine Ecology Progress Series. 2003; 249:15–24.

Bargu S, White JR, Li C, Czubakowski J, Fulweiler RW. Effects of freshwater input on nutrient loading, phytoplankton biomass, and cyanotoxin production in an oligohaline estuarine lake. Hydrobiologia. 2011; 661:377–389.

Berlman, I. Handbook of florescence spectra of aromatic molecules. Elsevier; 2012.

Bianchi TS, Cook RL, Perdue EM, Kolic PE, Green N, Zhang Y, et al. Impacts of diverted freshwater on dissolved organic matter and microbial communities in Barataria Bay, Louisiana, USA. Marine Environmental Research. 2011; 72:248–257. [PubMed: 22000271]

Chao, X., Hossain, AA., Jia, Y. Numerical modeling of flow and sediment transport in Lake Pontchartrain due to flood release from Bonnet Carré Spillway. INTECH Open Access Publisher; 2013.

Coble PG. Characterization of marine and terrestrial DOM in seawater using excitation-emission matrix spectroscopy. Marine Chemistry. 1996; 51:325–346.

Coble PG, Del Castillo CE, Avril B. Distribution and optical properties of CDOM in the Arabian Sea during the 1995 Southwest Monsoon. Deep Sea Research Part II: Topical Studies in Oceanography. 1998; 45:2195–2223.

Cook RL, Birdwell JE, Lattao C, Lowry M. A multi-method comparison of Atchafalaya Basin surface water organic matter samples. Journal of Environmental Quality. 2009; 38:702–711. [PubMed: 19244491]

Cory RM, McKnight DM. Fluorescence spectroscopy reveals ubiquitous presence of oxidized and reduced quinones in dissolved organic matter. Environmental Science & Technology. 2005; 39:8142–8149. [PubMed: 16294847]

Fichot CG, Benner R. The spectral slope coefficient of chromophoric dissolved organic matter (S275–295) as a tracer of terrigenous dissolved organic carbon in river-influenced ocean margins. Limnology and Oceanography. 2012; 57:1453–1466.

Ghisaidoobe AB, Chung SJ. Intrinsic tryptophan fluorescence in the detection and analysis of proteins: a focus on Förster resonance energy transfer techniques. International Journal of Molecular Sciences. 2014; 15:22518–22538. [PubMed: 25490136]

Ghosh S, Leff LG. Impacts of labile organic carbon concentration on organic and inorganic nitrogen utilization by a stream biofilm bacterial community. Applied and Environmental Microbiology. 2013; 79:7130–7141. [PubMed: 24038688]

Hernes PJ, Spencer RG, Dyda RY, Pellerin BA, Bachand PA, Bergamaschi BA. The role of hydrologic regimes on dissolved organic carbon composition in an agricultural watershed. Geochimica et Cosmochimica Acta. 2008; 72:5266–5277.

Huguet A, Vacher L, Relexans S, Saubusse S, Froidefond J-M, Parlanti E. Properties of fluorescent dissolved organic matter in the Gironde Estuary. Organic Geochemistry. 2009; 40:706–719.

Kolic PE, Roy ED, White JR, Cook RL. Spectroscopic measurements of estuarine dissolved organic matter dynamics during a large-scale Mississippi River flood diversion. Science of the Total Environment. 2014; 485:518–527. [PubMed: 24747244]

McKnight DM, Boyer EW, Westerhoff PK, Doran PT, Kulbe T, Andersen DT. Spectrofluorometric characterization of dissolved organic matter for indication of precursor organic material and aromaticity. Limnology and Oceanography. 2001; 46:38–48.

Mossa J. Sediment dynamics in the lowermost Mississippi River. Engineering Geology. 1996; 45:457–479.

Murphy KR, Butler KD, Spencer RG, Stedmon CA, Boehme JR, Aiken GR. Measurement of dissolved organic matter fluorescence in aquatic environments: an interlaboratory comparison. Environmental Science & Technology. 2010; 44:9405–9412. [PubMed: 21069954]

Murphy KR, Stedmon CA, Graeber D, Bro R. Fluorescence spectroscopy and multi-way techniques. PARAFAC Analytical Methods. 2013; 5:6557–6566.

Murphy KR, Stedmon CA, Wenig P, Bro R. OpenFluor–an online spectral library of auto-fluorescence by organic compounds in the environment. Analytical Methods. 2014; 6:658–661.

Ohno T, Bro R. Dissolved organic matter characterization using multiway spectral decomposition of fluorescence landscapes. Soil Science Society of America Journal. 2006; 70:2028–2037.

Parlanti E, Wörz K, Geoffroy L, Lamotte M. Dissolved organic matter fluorescence spectroscopy as a tool to estimate biological activity in a coastal zone submitted to anthropogenic inputs. Organic Geochemistry. 2000; 31:1765–1781.

Riekenberg J, Bargu S, Twilley R. Phytoplankton community shifts and harmful algae presence in a diversion influenced estuary. Estuaries and Coasts. 2015; 38:2213–2226.

Roy ED, White JR. Nitrate flux into the sediments of a shallow oligohaline estuary during large flood pulses of Mississippi River water. Journal of Environmental Quality. 2012; 41:1549–1556. [PubMed: 23099947]

Roy ED, White JR, Smith EA, Bargu S, Li C. Estuarine ecosystem response to three large-scale Mississippi River flood diversion events. Science of the Total Environment. 2013; 458:374–387. [PubMed: 23685135]

Seitz WR. Fluorescence methods for studying speciation of pollutants in water: fluorescence quenching yields information on the binding of metal ions to humic substances. Fluorescence polarization may be used to study the conformation of humics and the binding of organic pollutants to them. TrAC Trends in Analytical Chemistry. 1981; 1:79–83.

Stedmon CA, Markager S. Tracing the production and degradation of autochthonous fractions of dissolved organic matter by fluorescence analysis. Limnology and Oceanography. 2005; 50:1415–1426.

USACE (United States Army Corps of Engineers). Spillway operations information. 2016. http://www.mvn.usace.army.mil/ (accessed June 7, 2016)

USEPA (United States Environmental Protection Agency). Methods of chemical analysis of water and wastes. USEPA 600/R-93/100Cincinnati: Environmental Monitoring Support Laboratory; 1993.

USGS (United States Geological Survey). National Water Informatino Systyem. 2016. https://waterdata.usgs.gov/usa/nwis/uv?07376000 (accessed June 15, 2016)

Weishaar JL, Aiken GR, Bergamaschi BA, Fram MS, Fujii R, Mopper K. Evaluation of specific ultraviolet absorbance as an indicator of the chemical composition and reactivity of dissolved organic carbon. Environmental Science & Technology. 2003; 37:4702–4708. [PubMed: 14594381]

Weston NB, Joye SB. Temperature-driven decoupling of key phases of organic matter degradation in marine sediments. Proceedings of the National Academy of Sciences of the United States of America. 2005; 102:17036–17040. [PubMed: 16286654]

White J, Fulweiler R, Li C, Bargu S, Walker N, Twilley R, et al. Mississippi River flood of 2008: Observations of a large freshwater diversion on physical, chemical, and biological characteristics of a shallow estuarine lake. Environmental Science & Technology. 2009; 43:5599–5604. [PubMed: 19731650]

Zehr JP, Ward BB. Nitrogen cycling in the ocean: new perspectives on processes and paradigms. Applied and Environmental Microbiology. 2002; 68:1015–1024. [PubMed: 11872445]

Highlights

- Winter flood pulse delayed estuarine carbon cycling
- Source identification of dissolved organic matter using spectroscopic methods
- Separated abiotic from biological carbon transformations
- Increasing winter river flood pluses may impact estuarine food web dynamics

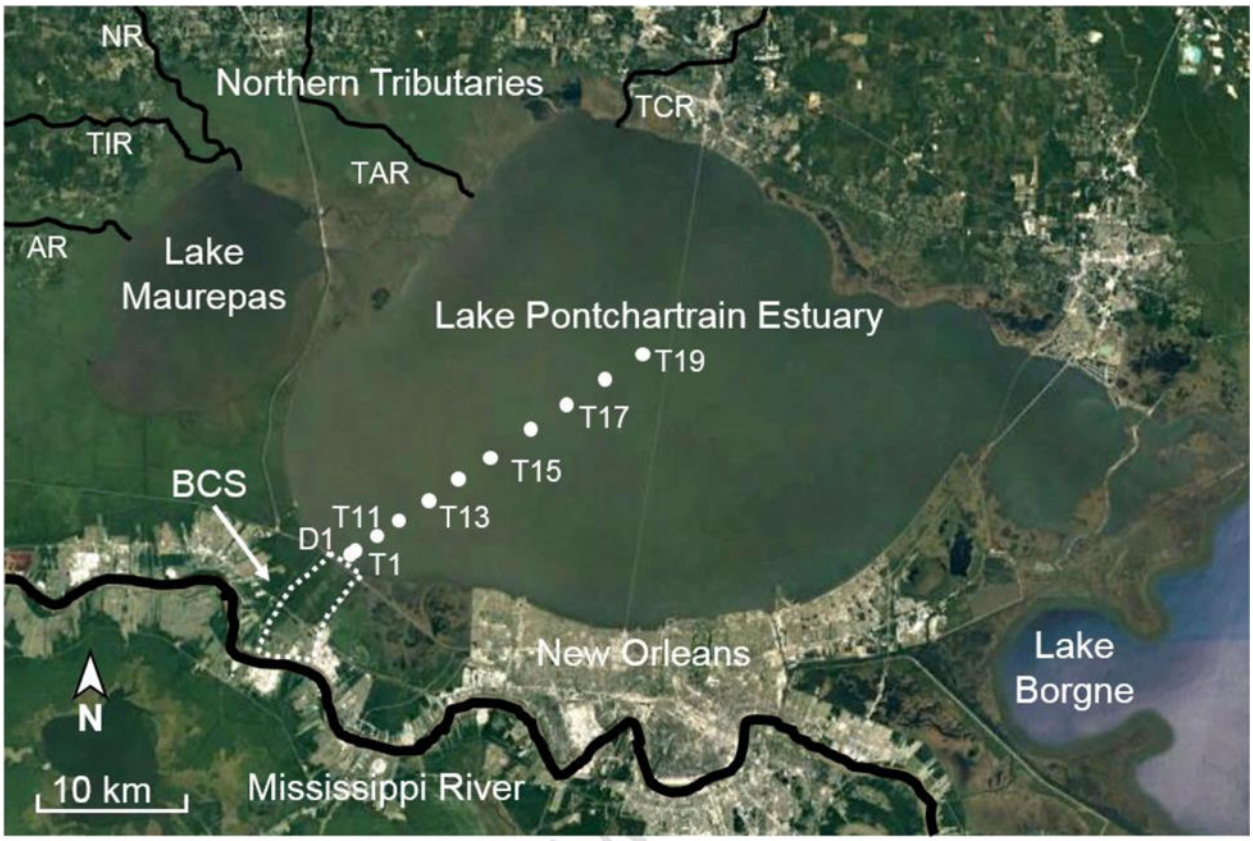

Figure 1.

Satellite image of Lake Pontchartrain Estuary, Mississippi River, Bonnet Carré Spillway (BCS) northern tributaries, and sites along the transect shown by the circles. Northern Tributaries consisting of the Lake Maurepas tributaries Amite River (AR), Tickfaw Rivers (TIR), and Natalbany River (NR) and Lake Pontchatrain Estuary tributaries Tangipahoa River (TAR) and Tchefuncte River (TCR) are outlined in the top left section of the figure.

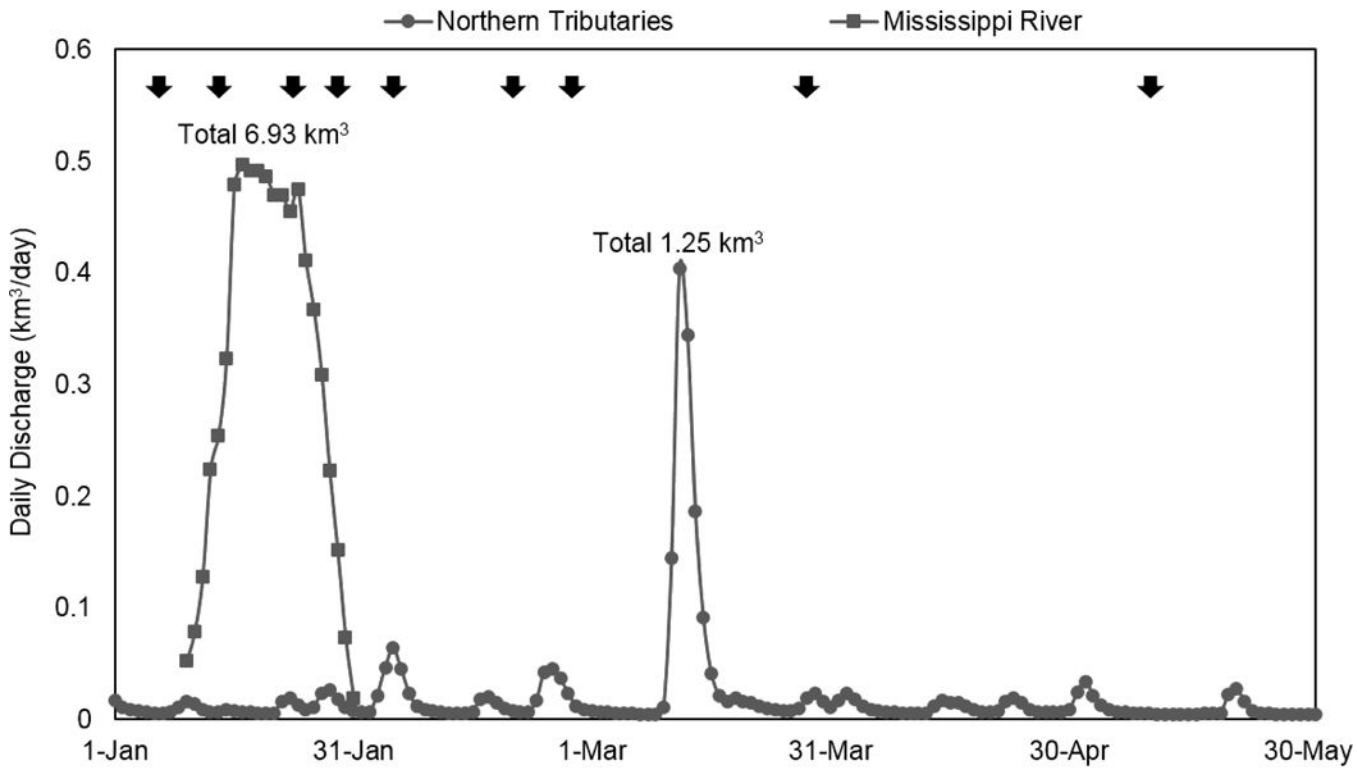

Figure 2.

Daily discharge of Mississippi River and northern tributaries from January 1 through May 30, 2016, with the individual sampling days indicated with arrows.

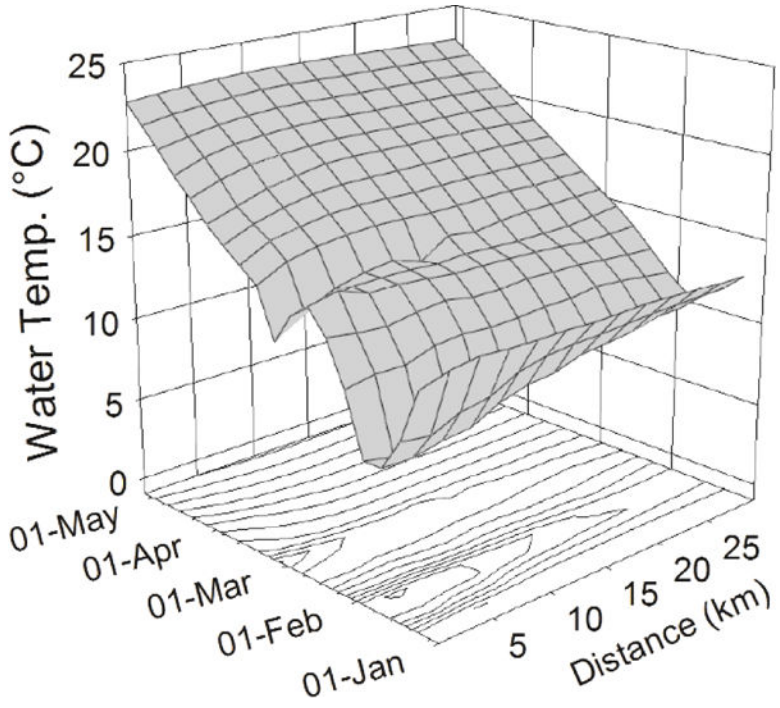

Figure 3.

Bisquare interpolated, three-dimensional plot with projected contours on the xy-plan, of water temperature (°C), by sampling date and distances from the Bonnet Carré Spillway.

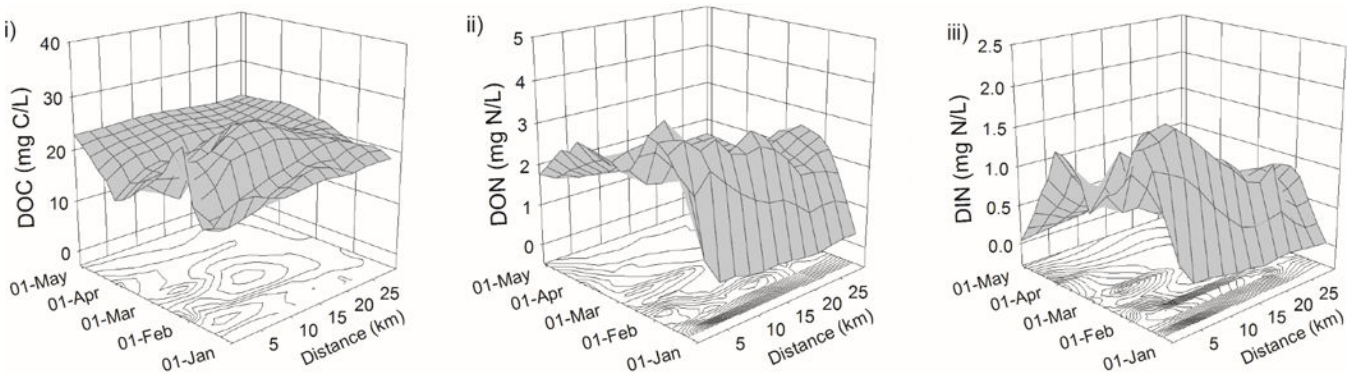

Figure 4.

Bisquare interpolated, three-dimensional plot with projected contours on the xy-plan, of: i) dissolved organic carbon (DOC), ii) dissolved organic nitrogen (DON), and iii) dissolved inorganic nitrogen (DIN), by sampling date and distances from the Bonnet Carré Spillway.

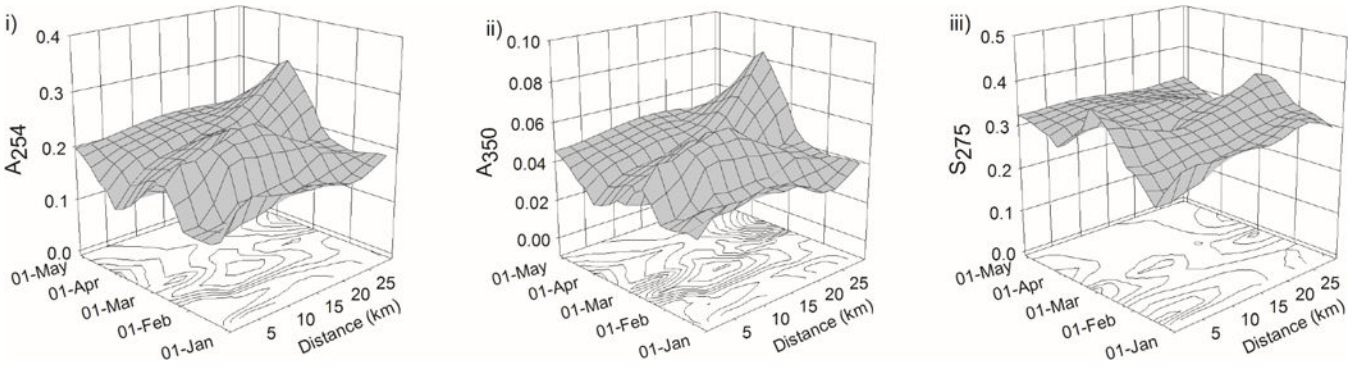

Figure 5.

Bisquare interpolated, three-dimensional plot with projected contours on the xy-plan, of ultraviolet-visible spectroscopy indicators: i) absorbance at 254 nm (A_{254}), ii) absorbance at 350 nm (A_{350}), and iii) spectral slope from 275 - 295 nm (S_{275}), by sampling date and distances from the Bonnet Carré Spillway.

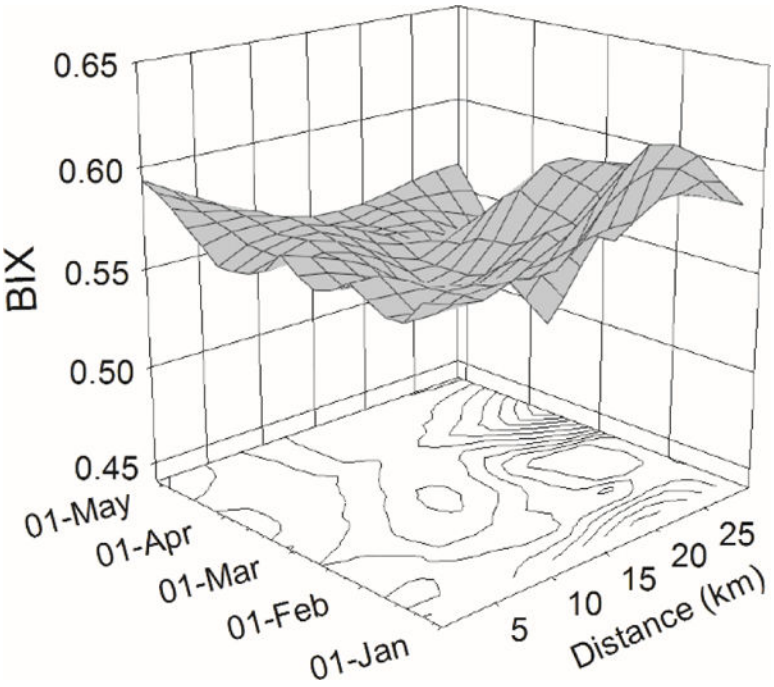

Figure 6.

Bisquare interpolated, three-dimensional plot with projected contours on the xy-plan, of the fluorescence spectroscopy indicator, biological index (BIX), by sampling dates and distances from the Bonnet Carré Spillway.

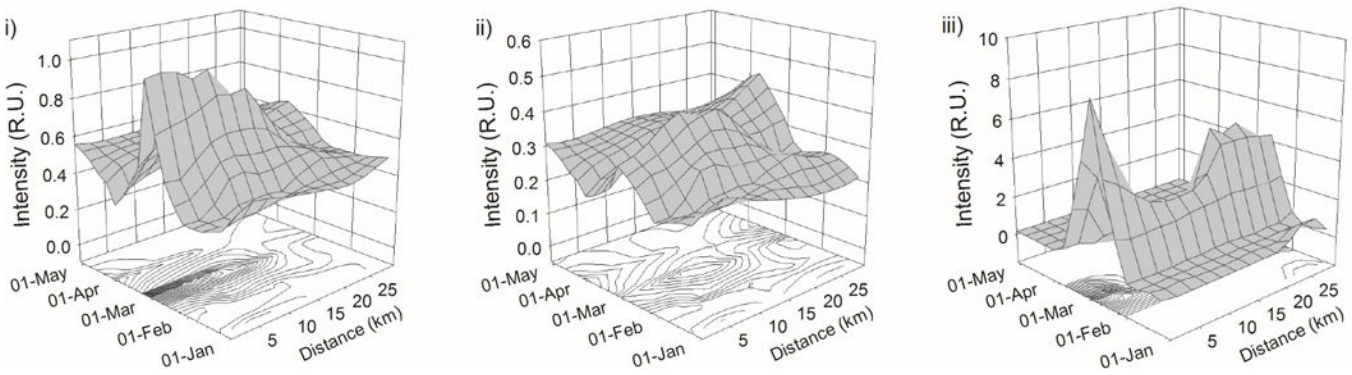

Figure 7.

Bisquare interpolated, three-dimensional plot with projected contours on the xy-plan, of PARAFAC determined fluorophores F_{max} intensity (Raman unites (R.U.): i) Fluorophore A, ii) Fluorophore T, and iii) Fluorophore B, by sampling date and distances from the Bonnet Carré Spillway (note the different interpolation of Figure 7iii)

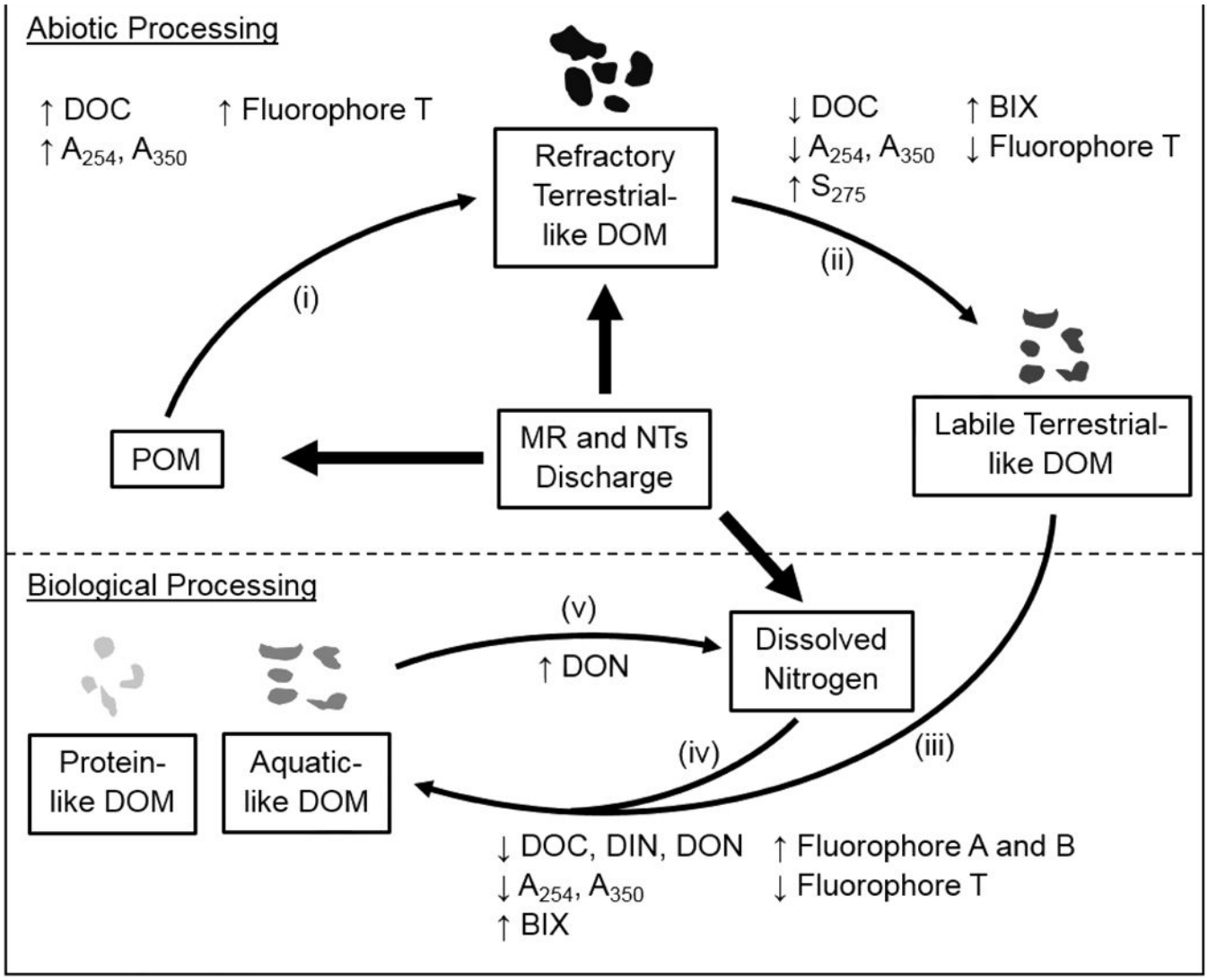

Figure 8.

Synthesis diagram of carbon cycling processes occurring in response to the Mississippi River (MR) and northern tributaries (NTs) discharge into Lake Pontchartrain Estuary; abiotic processing, and biological processing. With dissolved carbon and nitrogen, UV-Vis, fluorescence, and PARAFAC indicators responses in value for each of the transformations as indicated by the small up and down arrows. Thick arrows indicate direct input from the MR and NTs discharge and thin arrows indicate the occurring transformation processes. Transformation (i) represents abiotic processing of MR-inputted particulate organic matter (POM) to refractory terrestrial-like dissolved organic matter (DOM). Transformation (ii) represents abiotic processing of refractory terrestrial-like DOM to labile terrestrial-like DOM. Transformations (iii) and (iv) represent biological consumption of labile terrestrial-like DOM and dissolved nitrogen, respectively, and the production of aquatic-like and protein-like sourced DOM. Transformation (v) represents feedback loop production of DON.

Table 1

Liquid phase indicators via UV-Vis, fluorescence EEMs, and PARAFAC spectroscopic data.

Measurement	Description	Chemical Information	Ecological Information	Reference
UV-Vis Indicators				
A_{254}	Absorbance at wavelength of 254 nm	Concentration of aromatic carbon fraction of DOM	Plant and biological inputs, concentration of chromophore materials	Bianchi et al., 2011
A_{350}	Absorbance at wavelength of 350 nm	Concentration of lignin-like carbon fraction of DOM	Terrestrial inputs only	Hernes et al., 2008
Spectral slope (S) 275	Linear fit of the log-linearized Napierian absorption coefficient spectrum from 275–295 nm with unites of nm^{-1}	Lignin-like compounds' molecular weight (MW), low values indicating lignin-like with high MW and high values indicate lignin-like with low MW	Photodegradation of DOM and transformation of lignin-like from high MW to low MW	Chao et al., 2013; Fichot and Benner, 2012; Weishaar et al., 2003
Fluorescence EEMs Indicators				
Biological index (BIX)	Dividing the emission intensity at 380 nm (protein-like) by that at 430 nm (biological-like) with 310 nm excitation	Freshness of DOM pool with high values indicating fresher recently produced material and low values indicating less fresh older material	How recent the biological activity associated with the DOM pool	Huguet et al., 2009
PARAFAC Component Indicators				
Fluorophore A (Ex/Em: 270 (310)/425 nm)	Combination of UV humic-like and aquatic-like (autochthonous sourced) material Related peaks A and M	Lower degree of conjugation and abundance of functional groups; aromatic, carboxyl, and hydroxyl	Aquatic-like sourced, recently produced material	Cook et al., 2009, Berlman, 2012; Coble, 1996; Parlanti et al., 2000; Seitz, 1981
Fluorophore T (Ex/Em: 270 (395)/490 nm)	Combination of visible humic-like and soil fluvic acid (allochthonous sourced) material Related peaks C and D	Increase conjugation and abundance of functional groups; aromatic, and hydroxyl carboxyl,	Terrestrial-like sourced, older material	Cook et al., 2009, Berlman, 2012; Coble, 1996; Parlanti et al., 2000; Seitz, 1981
Fluorophore B (Ex/Em: 275/300 nm)	Biological sourced DOM Related peaks B	Proteins-like DOM in system	Result of biological activity (i.e. exudation spillage of cell)	Coble, 1996; Ghisaidoobe and Chung, 2014

Sci Total Environ. Author manuscript; available in PMC 2019 September 01.

Table 2

Determination of DOM dominant source at each site; Lake Pontchartrain Estuary (LPE), Mississippi River (MR), and northern tributaries (NTs) and mixing MR/LPE, MR/NTs, and NTs/LPE based on visual inspection of satellite images in conjunction with UV-Vis, fluorescence EEMs, and PARAFAC spectroscopic measurements.

Site	(km)	Jan 8, 2016	Jan 15, 2016	Jan 24, 2016	Jan 29, 2016	Feb 5, 2016	Feb 19, 2016	Feb 26, 2016	Mar 25, 2016	May 5, 2016
D1	0.57	NA	MR*	MR*	MR*	MR*	MR*	MR*	NTs/LPE*	NA
T1	1.12	CC	MR*	MR*	MR*	MR*	MR*	MR*	NTs/LPE*	NTs/LPE*
T11	2.98	CC	MR*	MR*	MR*	MR*	MR*	MR*	NTs/LPE*	NTs/LPE*
T12	5.13	CC	MR*	MR*	MR*	MR*	MR*	MR*	NTs/LPE*	NTs/LPE*
T13	8.05	CC	MR*	MR*	MR*	NTs*	MR*	NTs*	NTs/LPE*	NTs/LPE*
T14	11.25	CC	MR*	MR*	MR*	NTs*	NTs*	NTs*	NTs/LPE*	NTs*
T15	14.54	CC	MR*	MR/NTs*	MR*	MR/LPE*	NTs*	NTs*	NTs/LPE*	NTs*
T16	18.54	CC	LPE*	MR*	NTs*	MR/LPE*	NTs*	MR*	NTs*	NTs*
T17	22.23	CC	LPE*	MR*	NTs*	MR/LPE*	LPE*	LPE*	NTs*	NTs*
T18	26.13	CC	LPE*	MR*	NTs/LPE*	MR/LPE*	LPE*	NA	NTs*	NTs/LPE*
T19	29.82	CC	LPE*	MR*	NTs/LPE*	MR/LPE*	LPE*	NA	NTs*	NTs/LPE*

*Statistically ($p<0.05$) different from the other DOM sources on each sampling day based on biological index (BIX) measurements.

NA, not applicable - Data not collected due to safety concerns resulting from weather conditions.

CC, cloud cover – Source identification could not be made.

Mississippi River (MR)
Lake Pontchartrain Estuary (LPE)
Northern Tributaries (NTs)
MR/LPE
MR/NTs
NTs/LPE

Table 3

DOM sources Lake Pontchartrain Estuary (LPE), Mississippi River (MR), and northern tributaries (NTs) mean values with standard deviation for UV-Vis, fluorescence EEMs, and PARAFAC indicators, based on pure dominated DOM during discharges.

DOM source	Spectral slope (S_{275}, (nm^{-1})	Biological index (BIX)	F_{max} Intensity Fluorophore A (R.U.)	F_{max} Intensity Fluorophore T (R.U.)
MR	0.269 ± 0.033 *	0.570 ± 0.005 *	0.369 ± 0.025 *	0.222 ± 0.017 *
LPE	0.307 ± 0.016 *	0.594 ± 0.019 *	0.449 ± 0.040 *	0.234 ± 0.031 *
NTs	0.320 ± 0.018 *	0.546 ± 0.019 *	0.628 ± 0.128 *	0.360 ± 0.043 *

* Significantly ($p<0.05$) different from the other sources.